Numerical Simulation of Coastal Flows with Passive Pollutant by Regularized Hydrodynamic Equations in Shallow Water Approximation

T. G. Elizarova[2] [a] and A. V. Ivanov[1] [b]

[1]*M. V. Lomonosov Moscow State University, Chair of Mathematics, Leninskie Gory 1, bld. 1, Moscow, 119991, Russia*
[2]*M. V. Keldysh Institute of Applied Mathematics of the RAS, Miusskaya sq. 4, Moscow, 125047, Russia*

Keywords: Shallow Water, Regularized Equations, Finite Volume Approximation, Pollutant Transport.

Abstract: The paper presents a short overview of regularized shallow water equations and a new variant of the regularized system for modelling impurities transfer. The examples of the extreme surges simulation in the Sea of Azov in September 2014 with real wind forcing are presented. The results of calculations are compared with observation data of hydrometeorological stations in Taganrog. An example of calculating a passive pollutant transfer using the new algorithm is also given. The numerical scheme presented in the work is efficient and easy to implement in the form of finite-volume algorithm.

1 INTRODUCTION

In the study of wave motion in coastal sea and ocean flows there is a practical interest in modelling water movement under an influence of wind loads and Coriolis forces in real bottom relief as well as an impurities and pollutant transfer. For small depths, the implementation of hydrodynamic equations in the shallow water approximation is convenient from the physical point of view and for the efficiency of numerical algorithm also.

A family of original numerical algorithms based on regularization, or smoothing, of hydrodynamic equations was proposed thirty years ago, e.g., (Elizarova, 2009; Sheretov, 2009; Chetverushkin, 1999).This approach, known as quasi gas dynamic (QGD) equations, was successfully implemented in the international open platform OpenFOAM as one of the computational nodes, thus extending its application to a vast range of practical gas dynamic and hydrodynamic simulations (Kraposhin et al., 2018). Recently this approach, named as regularized shallow water equations (RSWE), was extended to hydrodynamic equations in the shallow water approximation, that allows flow simulations in coastal zones (Bulatov and Elizarova, 2011; Saburin and Elizarova, 2016; Saburin and Elizarova, 2017; Saburin and Elizarova, 2018). Modifications of RSWE algorithm for a uni-

[a] https://orcid.org/0000-0001-6169-5270
[b] https://orcid.org/0000-0002-2052-3912

fied tsunami modelling beginning from the source of a tsunami wave up to its interaction with the coastline, was proposed (Elizarova and Ivanov, 2018a). Using the same background an algorithm for two-layer shallow water flows was constructed and tested (Elizarova and Ivanov, 2018b). Such flows arise due to differences in salinity or temperature in different flow layers.

It is known that the numerical simulation of the transport of impurities or other passive scalars – for example, salinity or temperature, is poorly stable, which is especially important for small diffusion coefficients of the scalars. The construction of numerical methods for modelling the distribution of impurities in shallow water has been the subject of many studies, for example, (Bristeau and Perthame, 2001; Audusse and Bristeau, 2003; Delis and Katsaounis, 2004; Chertock and Kurganov, 2004). One of the most popular ways to solve this problem consists in applying a specialized separate algorithm to solve the transport equation. However the solution of such a system of hydrodynamic equations together with a transport equation is non- homogeneous. The authors managed to construct a homogeneous algorithm for modelling the hydrodynamic equations together with the passive scalar transport equation by considering the system of equations as a united system and introducing a regularizator for a hydrodynamic system with a transport equation as a whole. An example of such regularization and the first attempt of a passive pollutant transfer modelling is presented below.

The paper is organized as follows. In the second section we present a short overview of regularized shallow water equations (RSWE) together with the new regularized equation for a pollutant transfer. The general features of the related numerical algorithm are shortly described. In order to illustrate the capabilities of the RSWE algorithm the numerical simulation of the Azov Sea circulation with extremal storm wind forcing taking place 2013 and 2014 years is presented in the section 3. Here a pollutant transfer is not taken into consideration. In section 4 an example of RSWE with pollutant transfer in a test configuration is shown. In section 5 the RSWE system for passive scalar transfer together with pollutant source is presented separately. Some conclusions are given at the end of the paper.

2 SHALLOW WATER EQUATIONS AND THEIR REGULARIZED FORM

We consider the transport of a passive pollutant by a flow modelled by the shallow water equations system:

$$\frac{\partial h}{\partial t} + \operatorname{div}(h\mathbf{u}) = 0, \tag{1}$$

$$\frac{\partial (h\mathbf{u})}{\partial t} + \operatorname{div}(h\mathbf{u} \otimes \mathbf{u}) + \nabla \frac{gh^2}{2} = -gh\nabla b, \tag{2}$$

$$\frac{\partial Ch}{\partial t} + \operatorname{div}(\mathbf{u}Ch) = \operatorname{div}(Dh\nabla C). \tag{3}$$

Here, $h(\mathbf{x},t)$ and $\mathbf{u}(\mathbf{x},t)$ are the depth and velocity vector of the water respectively, $b(\mathbf{x})$ describes the topography of the bottom, g is the acceleration due to gravity, $C(\mathbf{x},t)$ is the average pollutant concentration and D is the diffusion coefficient. Therefore $\xi(\mathbf{x},t) = h(\mathbf{x},t) + b(\mathbf{x})$ is the level of water surface (see Fig. 1).
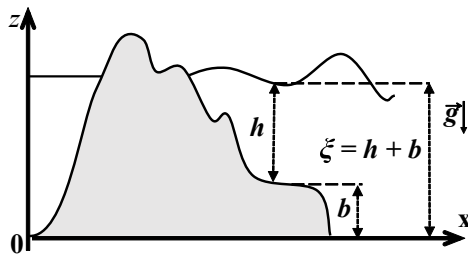
Figure 1: Schematic view of shallow water.

RSWE system, constructed on the base of (1)–(3) has the following form:

$$\frac{\partial h}{\partial t} + \operatorname{div}\mathbf{j_m} = 0, \tag{4}$$

$$\frac{\partial (h\mathbf{u})}{\partial t} + \operatorname{div}(\mathbf{j}_m \otimes \mathbf{u}) + \nabla \frac{gh^2}{2} = \tag{5}$$
$$= -gh^*\nabla b + \operatorname{div}\Pi,$$

$$\frac{\partial Ch}{\partial t} + \operatorname{div}(\mathbf{j}_m C) = \operatorname{div}(Dh\nabla C + \tau \mathbf{u}(\mathbf{u}h \cdot \nabla C)), \tag{6}$$

$$h^* = h - \tau \operatorname{div}(h\mathbf{u}), \tag{7}$$

$$\mathbf{j}_m = h(\mathbf{u} - \mathbf{w}), \tag{8}$$

$$\mathbf{w} = \frac{\tau}{h}\left[\operatorname{div}(h\mathbf{u} \otimes \mathbf{u}) + gh\nabla(b+h)\right], \tag{9}$$

$$\Pi = \tau \mathbf{u} \otimes \left[h(\mathbf{u} \cdot \nabla)\mathbf{u} + gh\nabla(b+h)\right] + \tag{10}$$
$$+ \tau I\left[gh\operatorname{div}(h\mathbf{u})\right].$$

Based on this system of equations, numerical algorithms are constructed.

The role of regularizing additives is performed here by the terms with a small parameter τ that has the dimension of a time. These additives allow the use of a finite-volume method with an approximation of all spatial derivatives using central differences. An explicit time-conditionally stable difference scheme is used, in which the time step has the same order of magnitude as τ. Therein τ is calculated as

$$\tau = \alpha \frac{l}{c}, \quad c = \sqrt{gh(\mathbf{x},t)}. \tag{11}$$

Here l is a characteristic dimension of spatial cells used in the numerical algorithm, c is the velocity of propagation of small disturbances calculated in the approximation of the shallow water model, $0 < \alpha < 1$ is a numerical coefficient based on conditions accuracy and stability. The time interval is chosen in accordance with the Courant condition:

$$\Delta t = \beta \frac{l}{c_{max}}. \tag{12}$$

The Courant number $0 < \beta < 1$ depends on parameter τ in the form $\beta = \beta(\alpha)$ and is chosen in the process of the calculations to ensure the monotonicity of the numerical solution.

Thus, the difference algorithm includes two configured parameters: Courant number β and coefficient α, which determine the accuracy and stability of the numerical solution.

3 AZOV SEA CIRCULATION WITH STORM WIND FORCING IN 2013 AND 2014 YEARS

Here we show the possibilities of numerical simulation of real coastal flows on RSWE system without taking into account pollutant transport.

The observations show that in the Sea of Azov, the impact of a long-term (for several days) unidirectional wind can generate a surface level gradient, whose destruction produces a seiche. This seiche is an analogue of a standing wave inside a pool.

The prediction of storm surges arising from the passage of extreme cyclones in the Black Sea region is of special interest in the forecast of the dynamics in the Azov Sea. Below we present an example of the modelling of seiche oscillations in the Azov Sea and flows caused by storm winds in March 2013 and September 2014 (Saburin and Elizarova, 2016; Saburin and Elizarova, 2017; Saburin and Elizarova, 2018). Here the algorithm includes the Coriolis force and quadratic friction on the bottom. Real wind effects are taken into account as forcing.

We consider a two-dimensional shallow water equations system in flux form. Taking into account external forces and the topology of the bottom, we can write the system in the following form:

$$\frac{\partial h}{\partial t} + \frac{\partial h u_x}{\partial x} + \frac{\partial h u_y}{\partial y} = 0, \tag{13}$$

$$\frac{\partial (h u_x)}{\partial t} + \frac{\partial}{\partial x}\left(h u_x^2 + \frac{1}{2}gh^2\right) + \frac{\partial}{\partial y}\left(h u_x u_y\right) = \tag{14}$$

$$= h f^c u_y - gh\frac{\partial b}{\partial x} + \tau^{x,w} - \tau^{x,b},$$

$$\frac{\partial (h u_y)}{\partial t} + \frac{\partial}{\partial x}\left(h u_x u_y\right) + \frac{\partial}{\partial y}\left(h u_y^2 + \frac{1}{2}gh^2\right) = \tag{15}$$

$$= -h f^c u_x - gh\frac{\partial b}{\partial y} + \tau^{y,w} - \tau^{y,b}.$$

Here $h(x,y,t)$ is the depth of the fluid, $u_x(x,y,t)$ and $u_y(x,y,t)$ are the components of the flow velocity, g is the acceleration of gravity, $f^c = 2\Omega\sin\varphi$ is the Coriolis parameter, where $\Omega = 7.2921\cdot 10^{-5}s^{-1}$ is the angular Earth rotation velocity, φ is the geographical latitude. The function $b(x,y)$ describes the topography of the bottom from a certain reference level positioned below the sea bottom (see Fig. 2).

The components of the wind friction force on the water surface are denoted by $\tau^w(x,y,t)$ and calculated as $\tau^{i,w}(x,y,t) = \gamma|W|W_i$, where $W_i(x,y,t)$ is the wind velocity component (m/s), $|W| = \sqrt{W_x^2 + W_y^2}$ is the

absolute value of the wind velocity, γ is the wind friction coefficient for the free water surface. The index i stands for x and y components.

The projections of the bottom friction are denoted by $\tau^b(x,y,t)$ and calculated with the use of the relation $\tau^{i,b}(x,y,t) = \mu|u|u_i$, where μ is the coefficient of friction, $|u| = \sqrt{u_x^2 + u_y^2}$ is the absolute value of the flow velocity.

The friction coefficients are the given values and for marine water areas are equal to $\mu = 2.6\cdot 10^{-3}$ and $\gamma = 0.001\frac{\rho_0}{\rho_w}(1.1 + 0.0004|W|)$, where $\rho_0 = 1.3\cdot 10^{-3}$ is the air density (g/cm^3), $\rho_w = 1.025$ is the water density (g/cm^3), the coefficient 0.0004 has the dimensionality $(m/s)^{-1}$.

The solution domain of the problem is the water area of the Azov Sea, the Kerch Strait, and the adjacent part of the Black Sea (see Fig. 2). It is located from $34°45'6''$ E to $39°29'38''$ E and from $44°48'4''$ N to $47°16'12''$ N, respectively. The topology of the bottom is given on a grid with the step $8''$, which corresponds to the spatial mesh size of 250 m.

Due to relatively small linear sizes of the considered water areas relative to the Earth radius, the problem is considered in the Cartesian system of coordinates. The equilibrium depth $h = h_0$ is chosen as initial conditions, which corresponds to the undisturbed sea level, and zero flow velocities $u_x = u_y = 0$ m/s. The boundary conditions along the shoreline use wet/dry bottom conditions. In the region of the Black Sea (Figure 2, lower border) where the boundary is placed along a grid line, we apply either drift conditions, or free boundary conditions in the normal direction to the boundary.
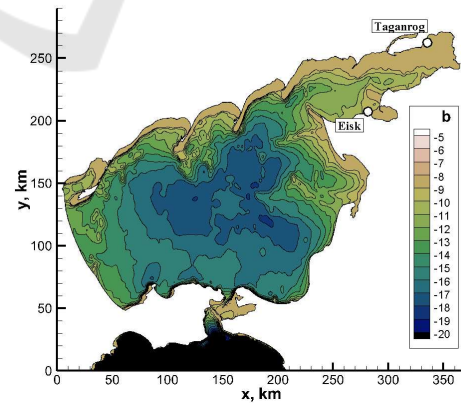
Figure 2: Bottom topography of the Azov Sea (m).

The external forcing was given in the form of wind flow velocity fields with the step of 1 hour calculated by the WRF model at the State Oceanographic Institute. The intervals of March 21–25, 2013 and September 21–25, 2014 were considered for analysis.

The circulation and sea level distributions at midnight 24 September 2014 are shown in fig. 3. The color upper left corner of the figure shows main stream lines of the wind. All characteristics correspond to a particular time moment indicated in the caption of the figure.
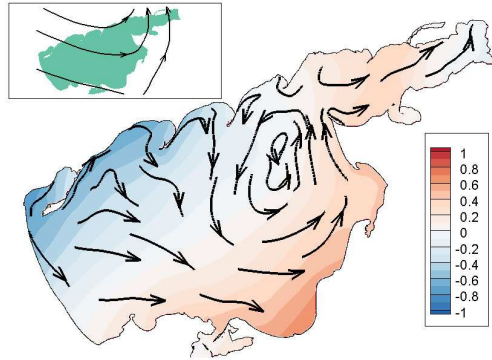
Figure 3: Deviation η of the sea level in the Azov Sea basin under storm surge on September 24, 2014. Calculations for $\mu = 0.00078$.

Here $\eta = h_0 - h(x,y,t)$ – deviation of the sea level. The color indicates the sea level relative to the equilibrium state, the arrows show stream lines.

Extreme surges of 2013 and 2014 have similar patterns of formation and it is possible to distinguish several stages in them. At the first stage the surges were preceded by an extreme outflow of water from the Taganrog Bay into the central part of the Azov Sea caused by south-east wind. The sea level in the Taganrog Bay dropped by -50 cm.

Further, within a few hours there was a sharp change of wind direction from south-east to south-west with hurricane-force wind gusts up to 32–37 m/s. After the change of wind direction, the circulation of the Azov Sea also changed and the surge of water began in the Taganrog Bay (fig. 3).

To analyse the effect of bottom friction on the solution to the problem and compare with real observation data, we consider the graph of sea level variation relative to the equilibrium state for different μ near the city of Taganrog. These are shown in Fig. 4 for 2014.

Figure 4 shows graph for the storm surge on September 21–25, 2014 in the city of Taganrog. For $\mu = 0$ the maximal height of surge was $h_{max} = 5.48$ m, the peak was attained at $t_{max} = 12 : 52$. For $\mu = 0.0026$ we have $h_{max} = 2.22$ m, $t_{max} = 16 : 15$, for $\mu = 0.00078$ we have $h_{max} = 3.12$ m, $t_{max} = 14 : 45$.

Thus, within the RSWE model the extreme surges of 2013 and 2014 in the Azov Sea were simulated. The general picture of formation of surges corresponds to the observation data. We compared the dynamics of the equilibrium sea level with the data
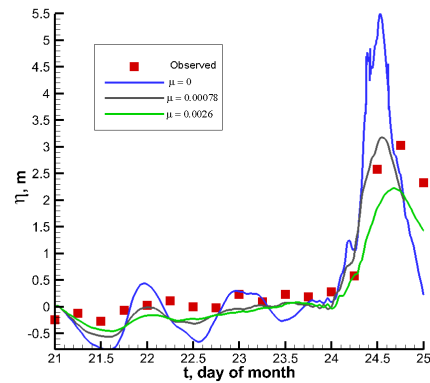
Figure 4: Time evolution of the sea level in the period of extreme surge on September 21–25, 2014 for the different coefficients of bottom friction city of Taganrog. The X axis corresponds to time t in days starting from September 21, the Y axis corresponds to the sea level deviation (m). Red squares indicate observations on the water level posts at these points.

of meteorological stations near the city of Taganrog. It was shown that the change of the bottom friction force affects both the height and time of the surge. For the extreme surge of 2014 we have chosen an optimal coefficient μ of bottom friction which reproduces the maximal height of the surge most accurately according to the data of meteorological observations.

4 TRANSPORT OF PASSIVE POLLUTANT

In this section the first example of numerical simulation of the pollutant transfer implying the numerical algorithm, based on the RSWE system, is demonstrated.

The test problem presents a pollutant transfer that takes place in dam break flow. The formulation of the problem is regarded according with (Chertock and Kurganov, 2004). The same test was also studied in (Delis and Katsaounis, 2004).

Here we consider a system with a flat bottom ($b(x,y) = 0$) in the square domain: $[0,1400]m \times [0,1400]m$ and the initial water depth and velocity distribution, that are shown in Fig. 5. The water flows from the left to the right through a breach located between $y = 560$ and $y = 840$. The initial concentration of pollutant is:

$$C(x,y,0) = \begin{cases} e^{-\frac{(x-650)^2+(y-600)^2}{10000}}, (x,y) \in D_1, \\ 0.5, (x,y) \in D_2, \end{cases} \quad (16)$$

where

$$D_1 = \{(x,y) : x \in [0,700], y \in [0,1400]\}, \quad (17)$$

$$D_2 = \{(x,y) : x \in [700,1400], y \in [0,1400]\}. \quad (18)$$
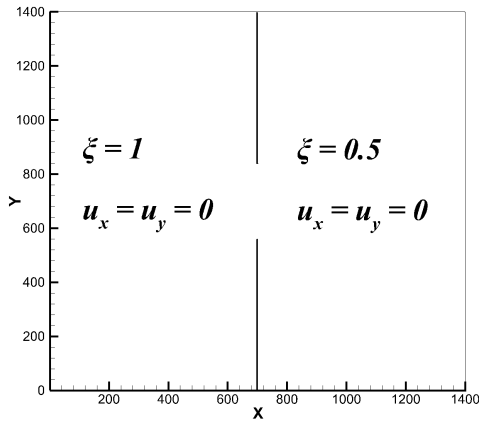
Figure 5: Initial conditions for the 2D dam break problem.

The boundary conditions at $x = 0$ and $x = 1400$m are assumed to be transmissive, or soft boundary conditions:

$$\frac{\partial h}{\partial \mathbf{n}} = 0, \quad \frac{\partial u_n}{\partial \mathbf{n}} = 0, \quad \frac{\partial u_\tau}{\partial \mathbf{n}} = 0, \quad (19)$$

and all the other boundaries are considered as reflective:

$$\frac{\partial h}{\partial \mathbf{n}} = 0, \quad u_n = 0, \quad \frac{\partial u_\tau}{\partial \mathbf{n}} = 0. \quad (20)$$

At the moment of dam breaking, water is released through the breach, forming a positive wave propagating downstream and a negative wave spreading upstream.
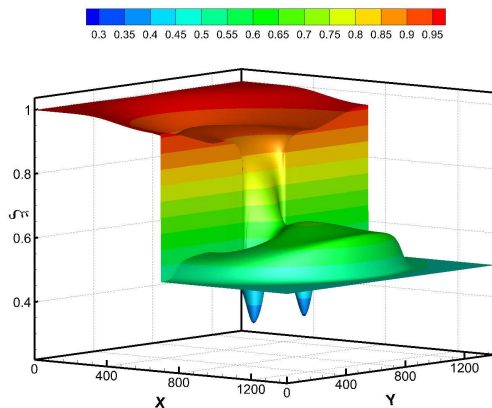
Figure 6: 2D dam break – 3D plot for the water height at $t = 200$s.

The solution is computed on a 500×500 grid, which corresponds to $\Delta x = \Delta y = 2.8$ m. The same grid was used in (Chertock and Kurganov, 2004; Delis and Katsaounis, 2004). The results at time $t = 200$s, with $\alpha = 0.5$, $\beta = 0.2$ is shown in Figs. 6 – 9. As one can observe, the scheme provides a very high resolution of the circular shock wave and the vortices formed on the breach (Fig. 6 and 7).

As α decreases to 0.2, the amplitude of the vortices increases, which corresponds to the picture presented in (Chertock and Kurganov, 2004; Delis and Katsaounis, 2004). Similarly for concentration – fig. 8 and 9 - one can observe a clear arrangement of the fronts and structures inside the vortices, as in (Chertock and Kurganov, 2004).
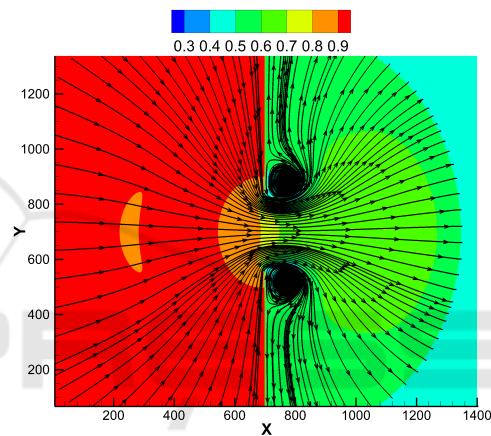
Figure 7: 2D dam break – Contour lines of h and streamlines at the time $t = 200$s.
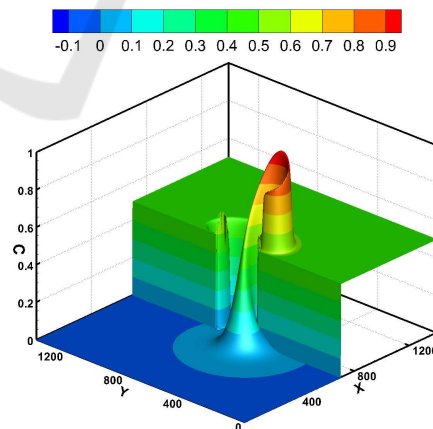
Figure 8: 2D dam break – 3D plot for the pollutant concentration $t = 200$s.

The mentioned examples show that numerical algorithm based on the RSWE system is comparable to the developed methods of the high order of accuracy.
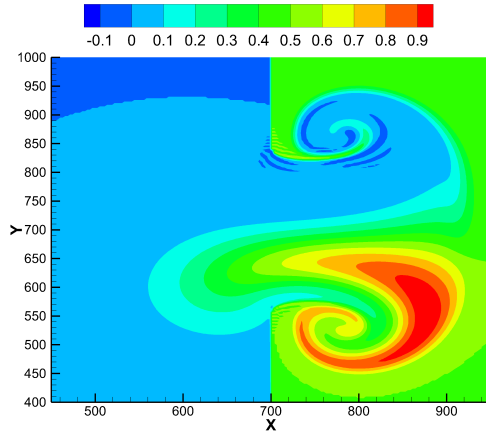
Figure 9: 2D dam break – top view for the pollutant concentration $t = 200s$.

5 TRANSPORT OF PASSIVE POLLUTANT WITH SOURCE TERM

The regularized system of shallow water equations including a transport equation with source term has the following form:

$$\frac{\partial h}{\partial t} + \operatorname{div} \mathbf{j_m} = S, \qquad (21)$$

$$\frac{\partial (h\mathbf{u})}{\partial t} + \operatorname{div} (\mathbf{j}_m \otimes \mathbf{u}) + \nabla \frac{gh^2}{2} = \qquad (22)$$
$$= -gh^* \nabla b + \operatorname{div} \Pi,$$

$$\frac{\partial Ch}{\partial t} + \operatorname{div} (\mathbf{j}_m C) = T_s S + \qquad (23)$$
$$+ \operatorname{div} (Dh\nabla C + \tau \mathbf{u} [(\mathbf{u}h \cdot \nabla C) + CS - T_s S]),$$

$$h^* = h - \tau (\operatorname{div} (h\mathbf{u}) - S), \qquad (24)$$

$$\mathbf{j}_m = h(\mathbf{u} - \mathbf{w}), \qquad (25)$$

$$\mathbf{w} = \frac{\tau}{h} [\operatorname{div} (h\mathbf{u} \otimes \mathbf{u}) + gh\nabla (b + h)], \qquad (26)$$

$$\Pi = \tau \mathbf{u} \otimes [h(\mathbf{u} \cdot \nabla) \mathbf{u} + gh\nabla (b + h) + S\mathbf{u}] + \qquad (27)$$
$$+ \tau I [gh (\operatorname{div} (h\mathbf{u}) - S)].$$

Here we imply the same notations as in the RSWE: $h(\mathbf{x}, t)$ and $\mathbf{u}(\mathbf{x}, t)$ are the depth and velocity vector of the water respectively, $b(\mathbf{x})$ describes the topography of the bottom, g is the acceleration due

to the gravity, $S(\mathbf{x}, t)$ denotes the sources of water, $C(\mathbf{x}, t)$ is an average pollutant concentration and T_s is a given value of a pollutant concentration at a sources S. D is the diffusion coefficient.

Introducing a source term in shallow water equation system causes a number of computational problems in numerical realizations, (Audusse and Bristeau, 2003) and (Delis and Katsaounis, 2004). Particularly, for a system of equations with a source term, it becomes necessary to preserve non-trivial equilibria, which is very difficult for most known schemes. One of the way to evaluate the influence of this factor on the solution, is the implementation of methods of an energy estimations of the solution, developed in (Zlotnik, 2012).

To demonstrate the performance of the RSWE system with source term we take the test problem from (Chertock and Kurganov, 2004), describing a propagation of the pollutant from a non-stationary source term in the region of the complex bottom topology.

Consider the square domain: $[0, 1400]m \times [0, 1400]m$ with the initial water depth and velocity distribution are shown in Fig. 10, where the shape of the dam is given by:

$$\Gamma(y) = \begin{cases} \min \left[500 + \frac{(y-700)^2}{400}, 900 \right], \\ \qquad\qquad\qquad y \in [0, 700], \\ 500, \quad 700 \leqslant y \leqslant 1400. \end{cases} \qquad (28)$$
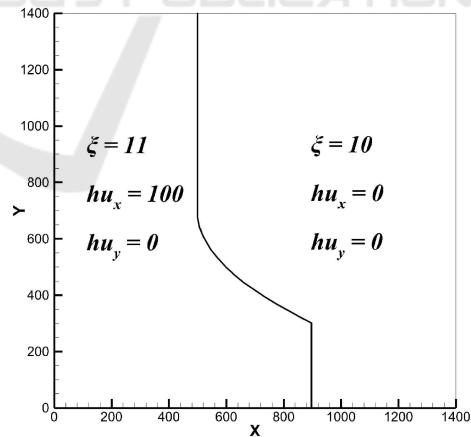
Figure 10: Initial conditions for the 2D dam break problem with non-zero source.

The bottom topography $b(x, y)$ is given by three elliptic-shape exponential humps:

$$b(x, y) = 4.5 \left[e^{-\kappa_1 (x-800)^2 - \kappa_2 (y-700)^2} + \qquad (29) \right.$$
$$\left. e^{-\kappa_2 (x-600)^2 - \kappa_1 (y-600)^2} + e^{-\kappa_2 (x-1000)^2 - \kappa_1 (y-700)^2} \right],$$

where $\kappa_1 = 10^{-4}$, $\kappa_2 = 10^{-3}$.

The initial concentration of pollutant is equal to zero $C(x, y, t = 0) = 0$, but later, when on a source of polluted water with the concentration of pollutant $T_s = 25$ is turned on:

$$S(x, y, t) = \tag{30}$$
$$= 0.5e^{-0.5(t-8)^2 - 10^{-5}(x+y-1300)^2 - 5 \cdot 10^{-4}(x-y-100)^2},$$

a pollutant begins to propagate in the domain.

The boundary conditions are considered as transmissive:

$$\frac{\partial h}{\partial \mathbf{n}} = 0, \quad \frac{\partial u_n}{\partial \mathbf{n}} = 0, \quad \frac{\partial u_\tau}{\partial \mathbf{n}} = 0, \tag{31}$$

The solution computed on a 500×500 grid, which corresponds to $\Delta x = \Delta y = 2.8$ m and $\alpha = 0.5$, $\beta = 0.2$ at time $t = 30$s is shown in Figs. 11–13.
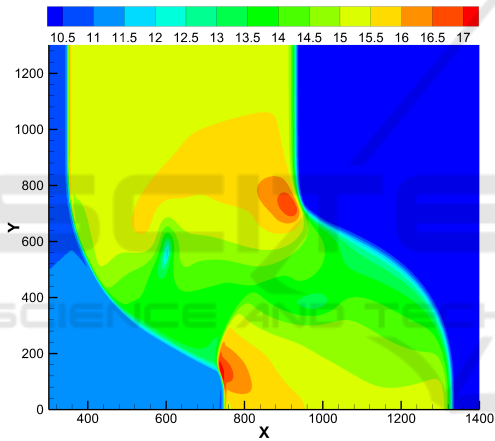
Figure 11: 2D dam break with non-zero source – a contour lines of ξ.
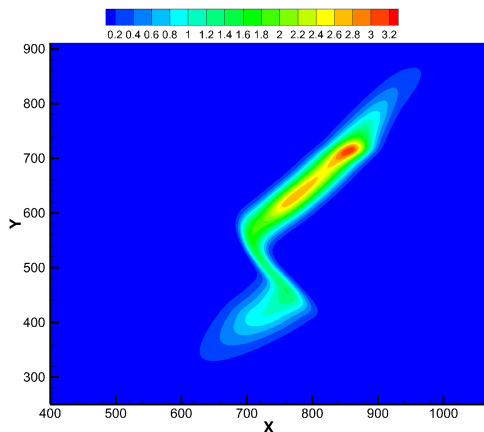
Figure 12: 2D dam break with non-zero source – a contour lines of C.
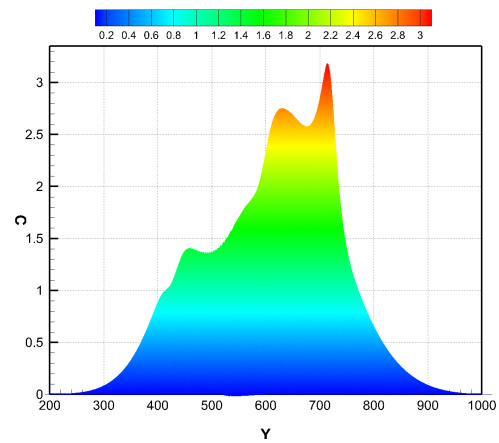
Figure 13: 2D dam break with non-zero source – 2-D projections of C.
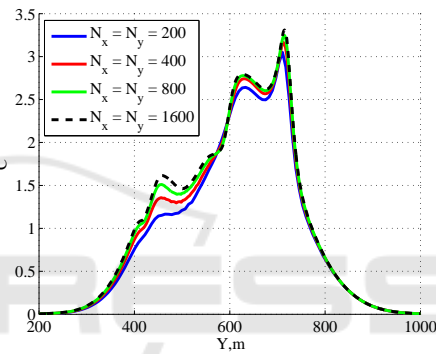
Figure 14: 2D dam break with non-zero source – 2-D projections of C for $\alpha = 0.5$, $\beta = 0.2$ and various partition of the grid.
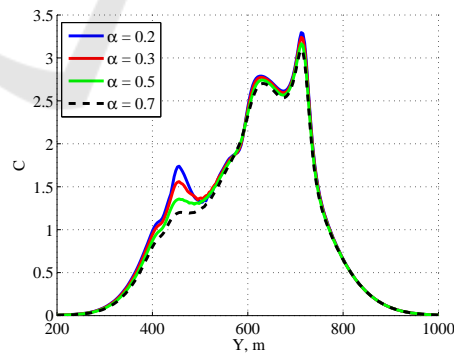
Figure 15: 2D dam break with non-zero source – 2-D projections of C for $N_x = N_y = 400$, $\beta = 0.2$ and various α.

In figure 11 one can observe that the collision of a curved shock wave of the initial distribution with bottom topography leads to rather complex wave structures.

Our results are compared with the semi-discrete central-upwind finite-volume(FV) scheme and the hy-

brid finite volume particle method (FVP) for partitioning on grid 500×500 in (Chertock and Kurganov, 2004).

The fig. 13 shows the results of calculations for the concentration in a 2D-projection on the (C, y) axis. The result obtained using the RSWE model was compared with the FV and FVP methods from (Chertock and Kurganov, 2004), and it was found that they are placed approximately between them.

The dependence of the numerical solution on the partition of the grid for the 2D-projection of C ($\beta = 0.2$, $\alpha = 0.5$) is shown in fig. 14. Fig. 15 demonstrates the 2D-projection of C ($N_x = N_y = 400$, $\beta = 0.2$) for the various α.

6 CONCLUSIONS

The regularized shallow water algorithm with proposed new method for pollutant transfer simulation has the similar structure as the methods of numerical solution of the subsonic and supersonic gas dynamics flows, already successfully implemented in the OpenFOAM platform (Kraposhin et al., 2018). The proposed algorithms in a form of finite-volume method can be included in the platform as a novel numerical solver for coastal flow simulations together with a pollutant transfer.

ACKNOWLEDGEMENTS

REFERENCES

Audusse, E. and Bristeau, M.-O. (2003). Transport of pollutant in shallow water a two time steps kinetic method. *ESAIM: M2AN*, 37:389–416.

Bristeau, M.-O. and Perthame, B. (2001). Transport of pollutant in shallow water using kinetic schemes. *ESAIM: Proc*, 10:9–21.

Bulatov, O. V. and Elizarova, T. G. (2011). Regularized shallow water equations and an efficient method for numerical simulation of shallow water flows. *Comput. Math. Math. Phys.*, 51:160–173.

Chertock, A. and Kurganov, A. (2004). On a hybrid finite-volume-particle method. *ESAIM: M2AN*, pages 1071–1091.

Chetverushkin, B. N. (1999). *Kinetically Consistent Schemes in Gas Dynamic*. Mosk. Gos. Univ., Moscow.

Delis, A. I. and Katsaounis, T. (2004). A generalized relaxation method for transport and diffusion of pollutant models in shallow water. *Computational Methods in Applied Mathematics*, 4:410–430.

Elizarova, T. G. (2009). *Quasi-Gas Dynamic Equations*. Springer-Verlag, Berlin.

Elizarova, T. G. and Ivanov, A. V. (2018a). On a homogeneous algorithm for numerical modeling of a tsunami wave. *Memoirs of the Faculty of Physics*, pages 1–6.

Elizarova, T. G. and Ivanov, A. V. (2018b). Regularized equations for numerical simulation of flows in the two-layer shallow water approximation. *Comput. Math. Math. Phys.*, 58(5):714–734.

Kraposhin, M. V., Smirnova, E. V., Elizarova, T. G., and Istomina, M. A. (2018). Development of a new OpenFOAM solver using regularized gas dynamic equations. *Computers & Fluids*, 166:163–175.

Saburin, D. S. and Elizarova, T. G. (2016). Numerical modeling of seiche oscillations in the sea of azov using smoothed hydrodynamic equations. In Konovalov, S. K., Korotaev, G. K., Ibraev, R. A., and Demishev, S. G., editors, *World Ocean: Models, Data and Operational Oceanology*, page 49—50.

Saburin, D. S. and Elizarova, T. G. (2017). Application of the regularized shallow water equations for numerical simulation of seiche level oscillations in the sea of azov. *Math. Models Comput. Simul*, 9(4):423–436.

Saburin, D. S. and Elizarova, T. G. (2018). Modelling the azov sea circulation and extreme surges in 2013-2014 using the regularized shallow water equations. russian journal of numerical analysis and mathematical modelling. *Russ. J. Numer. Anal. Math. Modelling*, 33(3):173–185.

Sheretov, Y. V. (2009). *Continuum Dynamics under Spatiotemporal Averaging*. NITs Regulyarnaya i Khaoticheskaya Dinamika, Moscow.

Zlotnik, A. A. (2012). "spatial discretization of the one-dimensional barotropic quasi-gasdynamic system of equations and the energy balance equation. *Mat. Model*, 24:51–64.